

Acid Blue 74 removal from aqueous solutions by EC/GAC coupling: a multi-objective optimization approach based on a hybrid NN-GA

Marius Sebastian Secula^a, George Ciprian Piuleac^a, Benoît Cagnon^{b,*}

^aDepartment of Chemical Engineering, Faculty of Chemical Engineering and Environmental Protection, TUIASI – “Gheorghe Asachi” Technical University of Iasi, 73 Prof. Dr. Doc. D. Mangeron, 700050, Iasi, Romania

^bInterfaces, Containment, Materials and Nanostructures (ICMN-UMR 7374), CNRS – University of Orleans, France, Tel. +33 238494431; Fax: +33 238494425; email: benoit.cagnon@univ-orleans.fr (B. Cagnon)

Received 13 May 2022; Accepted 5 August 2022

ABSTRACT

A hybrid approach based on neural networks and genetic algorithms was employed to develop a novel multi-objective procedure. Acid Blue 74 (AB74) removal by granular activated carbon/electrocoagulation (GAC/EC) coupling operated in alternating pulse current mode was investigated. Five independent variables, namely current density, GAC dose, initial pH value, initial AB74 concentration and GAC/EC time, were investigated. The dependent variables, that is, total organic carbon (TOC) removal efficiency, unit energy demand, and unit electrode material demands (Fe or Al), were considered. Six optimization cases are discussed by assuming different constraints. The optimal conditions for three imposed values of removal efficiency (80%, 90% and 97%) within the experimental region and at the highest level of GAC dose were analyzed. Under optimal conditions, 97% TOC removal efficiency was obtained for 0.2 g/L of dye solution by applying a current density of 86.9 A/m² for only 18.83 min and adding a GAC dose of 0.88 g/L.

Keywords: Electrocoagulation (EC); Coupling process; Multi-objective optimization; Acid Blue 74; Alternating pulse current; Neural networks-genetic algorithms (NN-GA)

1. Introduction

Due to their high toxicity, textile wastewaters are strictly regulated and have to be treated before being discharged into the environment [1]. Dyes are one of the most important classes of pollutants. A textile dye-stuff commonly used for dyeing cotton and wool fabrics [2], polyester fibers, and denim [3] is indigo carmine. To remove indigo carmine from wastewater, various methods such as adsorption [4], biological [2] and photochemical [5] techniques have been used. Precipitation-based processes are among the most appropriate and economical techniques [6]. Electrocoagulation (EC) is a well-known eco-friendly, simple, and efficient method for the treatment of dye-containing wastewater [7–11]. Although the electrical

operational costs of EC related to energy and electrode material consumption are crucial to evaluate the feasibility of a process, only a few studies have addressed the economical aspect of the EC technique [12].

The possibility of enhancing conventional EC systems by means of granular activated carbon (GAC) was recently suggested [13,14]. It has been proved that hybrid EC/GAC sorption systems are a more efficient and faster separation technique than conventional EC [13,14]. However, since electrocoagulation is a very complex process, modeling this process by means of statistical methods is preferred to an analytical modeling approach. Applied statistical mathematical approaches to EC over a wide parameter range have been shown to be more reliable for the design and scale-up of electrocoagulation reactors [15]. The rate

* Corresponding author.

of reaction in this kind of system is a non-linear function of temperature, current density, time, electrode type, etc. For all these reasons, the ability of neural networks (NN) and genetic algorithms (GA) to recognize and reproduce cause–effect relationships through training, for multiple input-output systems, could be employed to describe this process.

GAs are a search and optimization tool that is increasingly applied in scientific problems because it does not require any information about the search space, only an objective function that assigns a value to any solution. One choice for an optimization problem with a single or multiple targets that are often contrary is relatively complicated in the context of a precise mathematical model and high saved time resources requirements. This matter can be approached with scalar [16] or vector [17] objective functions. The combination of a GA and a NN involves procedures to identify the regions in the search domain [18]. Usually, the best data solutions given by GAs are implemented to optimize the uncertain baseline data obtained from NNs. The global optimum is a pseudo-global (deterministic) optimum and the closest solution of the pseudo-global optimum can be analyzed by the user.

In addition to increasing efficiency by reducing the calculation time, a hybrid procedure is not based on a specific mathematical structure, leading to a much simpler implementation. Hybrid search algorithms do not depend on the definition of the objective function and the characteristic quality of model predictions, but rather on a quantitative measure of the system, which can be used as a criterion in performance evaluation solutions [19].

If the process mechanisms are not fully known, conventional methods are not suitable. Many different situations are reported in the literature, considering single or multiple objective problems [20–23].

The present paper provides data concerning the removal of aqueous dye solutions by EC/GAC coupling. The experimental design also aimed at the development of a novel method for the quantitative assessment of the EC/GAC coupling process, and determination of the optimal electro-coagulant dose. The main goal was to combine in a novel manner a hybrid structure between a NN model and a GA so as to develop an efficient and effective multi-objective optimization procedure. Accurate results obtained for both modeling and optimizations, experimentally validated, prove the efficiency of the methodology. We have considered in the optimization approach the electrode material consumption, which is a very important cost factor for this method. In fact, the cost of electrode material consumed is up to ten times that of energy. Also, a detailed discussion on six different optimization cases and treatment costs has been provided. The cheapness feature of EC/GAC system is quantified.

2. Experimental

2.1. Materials

Acid Blue 74, with the commercial name indigo carmine, is a toxic indigoid dye named according to I.U.P.A.C. 3,3'-dioxo-2,2'-bis-indolyden-5,5'-disulfonic acid disodium salt ($C_{16}H_8O_8N_2S_2Na_2$). Its molecular structure is presented by

the study of Secula et al. [14]. It has a molecular weight of 466.36 g/mol, a color index number of 73015 and a maximum light absorption at 612 nm.

The GAC material used in this study was of commercial type L27 (Jacobi Carbons, France). Before use, the adsorbent was washed several times with water and then dried at 120°C for 24 h to remove residual acidity due to the activation protocol. The textural and chemical characteristics of this adsorbent material are described by the study of Secula et al. [14].

Solutions of Acid Blue 74 of 1 L volume were prepared before each experimental run by dissolving precisely-weighed amounts of dye (Sigma-Aldrich) in ultra-purified water (resistivity of 18.2 MW/cm at 25°C). NaCl (A.R. Lachner, Neratovice, Czech Republic) was used as background electrolyte.

To ensure a proper conductivity, 1.5 g of NaCl was dissolved in 1 L of synthetic dye solution. In prior work Secula et al. [24], it was determined that this is the optimal concentration of supporting electrolyte.

2.2. Procedure and analyses

EC experimental tests were conducted in a two-plane electrode cell. Based on our prior studies [24], it was established that a combined Al–Fe electrode configuration achieves the best performance for Acid Blue 74 removal as the obtained flocks are more stable and the separation is enhanced. A thorough analysis of the formed sludge during EC treatment of IC aqueous solutions was provided in our prior study [25]. Due to certain advantages such as electrode “self-cleaning” [25], removal efficiency [26] and lower energy consumption, the EC reactor was operated in alternating pulse current (APC) mode. The experimental set-up and procedures were described by the study of Secula et al. [14]. For the present study (Fig. 1), the electrodes were connected to an automatic polarity changer connected in the electrical circuit composed of the EC cell and a direct current (DC) power supply (IT6322, 0–30 V; 0–3 A; ITECH, Nanjing, China).

By means of APC, a contaminated cathode was transformed into a soluble anode, and then cleaned through anodic dissolution (allowing the accurate dosing of Al and Fe ions, respectively). Fig. 2 shows how the cell voltage varies when operated in APC mode. In this operating regime, the polarity of the electrodes was changed every 5 min thus favoring the “self-cleaning” of the electrodes. A VC530 VOLTCRAFT Data Logger Multimeter, connected to a PC, was used to measure the cell voltage with one reading per second. Solution pH and electrical conductivity were measured by means of a PC-connected C863 Consort multi-parameter analyzer.

The electrodes were weighed before and after EC by means of an Acculab ATL-224-I analytical digital balance (accuracy 0.1 mg) to estimate the amount of dissolved material. All the runs were performed at a room temperature of 25°C ± 1°C.

A volume of approximately 3 mL of sample was taken, allowed to settle, filtrated by means of Whatman 0.45 µm filters, and then analyzed.

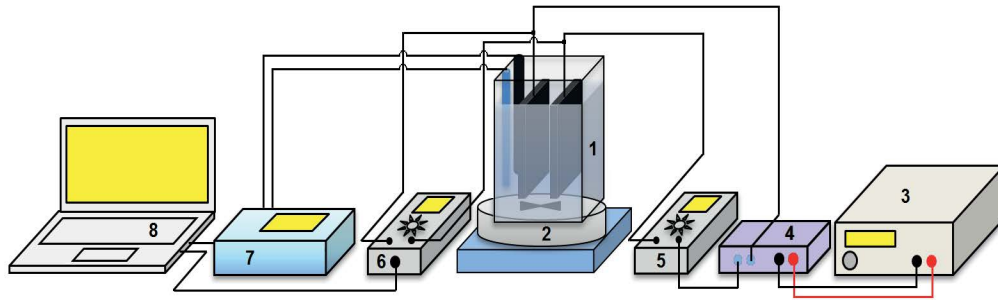


Fig. 1. Experimental set-up operated in alternative pulsed current (APC) mode. [1-EC cell; 2-magnetic stirrer; 3-direct current (DC) power supply; 4-polarity changer; 5-ammeter; 6-data logging voltmeter; 7-multi-parameter analyzer; 8-computer].

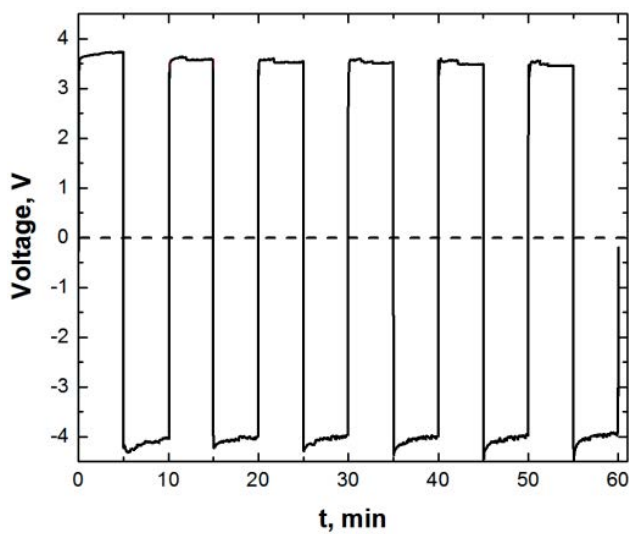


Fig. 2. Evolution of voltage during EC conducted under alternating rectangular pulse current as measured by means of the data logging voltmeter.

The removal efficiency was determined in terms of total organic carbon (TOC). TOC analysis was performed through combustion of samples at 680°C using a Multi N/C 2100/2100S Analytik Jena Analyzer.

2.3. Determination of responses

The TOC removal efficiency Y (%) was calculated using Eq. (1):

$$Y = \frac{TOC_i - TOC_t}{TOC_i} \times 100 \quad (1)$$

where TOC_i is the total organic content before treatment (mg/L), and TOC_t is the total organic content after t minutes of treatment (mg/L).

The consumption of electrical energy and electrode material represents the main cost of the electrocoagulation technology.

In order to optimize the investigated EC system in relation to electrical energy consumption, the specific energy

consumption or unit energy demand (UED, kWh/kg) [27] was determined according to Eq. (2):

$$UED = \frac{\left(I \cdot \int_0^t U \cdot dt \right)}{\left(1000 \cdot V \cdot TOC_i \cdot \frac{Y_t}{100} \right)} \quad (2)$$

where U is the cell voltage, (V), I – current intensity, (A), t – time, (h), V – volume of treated solution, (m³), Y_t – TOC removal efficiency at time t , (%).

The generation of coagulant during the EC process can be estimated by means of Faraday’s law [28]. However, the values of electrode-mass dissolved were found to be considerably higher than those predicted by Faraday’s law, especially in the case of aluminum electrodes. This is in agreement with data reported in the literature [29]. Therefore, in order to determine accurately the amount of ion dissolved, a correction factor must be used [30] as shown in Eq. (3):

$$UEMD_M = \frac{I \cdot t \cdot A}{\left[f \cdot n \cdot F \cdot V \cdot TOC_i \cdot \left(\frac{Y_t}{100} \right) \right]} \quad (3)$$

where $UEMD_M$ is the unit electrode material (Al or Fe, according to the APC applied) demand, (kg/kg); t – time, (s); n – number of electrons involved in the oxidation/reduction reaction; F – Faraday’s constant, (C/mol); A – atomic mass of electrode material, (g/mol); f – ratio of electrochemical dissolution.

Electrical operational costs (EOCs) of the EC dye wastewater can be calculated by means of Eq. (4) on the basis of the amount of energy and materials consumed [30,31]:

$$EOC = EEC + EMC = UED \cdot EEP + UEMD_{Fe} \cdot EMP_{Fe} + UEMD_{Al} \cdot EMP_{Al} \quad (4)$$

where EOC is the electrical operating cost of TOC removed, (€/kg); EEC – electrical energy consumption of dye, (€/kg); EEP – electrical energy price, (€/kWh); EMC – electrode material cost, (€/kg); EMP – electrode material price, (€/kg).

2.4. Soft-computing strategy for modeling and optimization

Genetic algorithms (GAs) are stochastic optimization techniques based on an intelligent mechanism that mimics natural selection. The GA starts with an initial set of solutions called initial population. Each solution of the population is represented by a chromosome (or individual) that is a point in the searching area. Chromosomes are developed through successive iterations, or generations, by genetic operators (selection, recombination, and mutation) that mimic the principles of natural evolution. Population size, number of generations, crossover probability and mutation are the control parameters of GAs. The values of these parameters must be specified before executing the GA and depend on the nature of the objective function. To solve the GA, it is important to adjust its parameters according to the particular problem addressed, so as to obtain good solutions and avoid premature convergence.

The selection operator chooses some “good” solutions and the recombination operator (crossover) generates new solutions, retaining the best characteristics of parents, while the mutation operator enhances diversity and seeks a way to avoid local minima [32]. In a GA, the fitness function value (optimization of the objective function) is adjusted to each individual according to the requirements of the task. Generation after generation, new individuals, called offspring, are created, and the chromosomes of the current population, called parents, forming a new population randomly.

To solve a multi-objective function-based vector component, a multi-objective problem can be reduced to a vector [17] or a scalar format [16]. In optimization problems operating with scalar functions, two methods can be used: (i) considering a single objective and treating the other objectives as constraints; (ii) using all the targets in a single objective function by using weighting factors.

Both approaches allow the use of simple algorithms, but the solution depends on the structure of the problem. For the first approach, the disadvantage seems to lie in the choice of the optimized function and the associated constraints. In the second case, assigning values of weighting factors, often arbitrarily, is a drawback of the method. Furthermore, the aggregation of all the objectives in a single function involves mixing different quantities, such as cost, quality, and environmental effects in a common unit. A major disadvantage is that the optimal solution of the scaling can be lost if a dual gap in the objective function convexity is created [33].

The multi-objective problem deals with more than one objective function at a time. The number of constraints must be satisfied by a feasible solution. Generally, the optimization problem is represented as follows:

minimize/maximize: $[f_1(x), f_2(x), \dots, f_n(x)]$, $n = 1, 2, \dots, N$;

subjected to: $g_k(x) = 0$, $k = 1, 2, \dots, K$;

$h_j(x) \geq 0$, $j = 1, 2, \dots, J$;

$x_i^L \leq x_i \leq x_i^U$, $i = 1, 2, \dots, m$.

where $g_k(x)$ and $h_j(x)$ are the problem constraints; solution x is a vector from m decision variables: $x = (x_1, x_2, \dots, x_m)^T$. The last set of constraints is called variable bounds, restricting each decision variable x_i to values within a lower x_i^L and upper x_i^U bound [34].

Neural networks (NNs), the dominant paradigm of artificial intelligence, are signal processing systems composed of a large number of interconnected elementary processors called artificial neurons or nodes that cooperate together to solve specific tasks. A given engineering problem may contain a mixture of types of decision variables (numbers, symbols, and other structural parameters). Since evolutionary algorithms operate on genetic coding of optimized variables, NNs can be used with multiple types of variables.

Like the main evolutionary algorithms, GAs are iterative processes by which a population is initialized in a random manner and then successively transformed by selection, mutation and crossover, until a certain number of iterations (generations) or until the completion of another stopping criterion.

The main goal of this work is to develop a general procedure based on neural networks and a GA which could be applied to the complex multi-objective optimization problem of an electrocoagulation process applied to wastewater treatment. NNs are used as an efficient modeling tool and GA as solving method of optimization using a multi-objective problem.

3. Results and discussion

Twenty-seven runs were performed in order to establish the functional relationships between the five independent variables (current density, GAC dose, initial pH value, initial AB74 concentration and GAC/EC time) and the considered responses. For each experimental run, nine samples were analyzed at certain durations of the GAC/EC coupling process.

The influence of the five factors on the responses was first investigated by one-at-a-time experiments. The runs consisted in varying a single factor while keeping the others constant. Fig. 3 shows the main effects of current density, GAC dose, and initial concentration of dye, pH and time on the TOC removal efficiency, UED, $UEMD_{Fe}$ and $UEMD_{Al}$ responses.

Fig. 3a shows the effect of current density on the four responses. For a dye concentration of 0.6 g/L, a TOC removal efficiency of 95.5% was obtained after 25 min of processing at 75.13 A/m², pH of 6 and a GAC dose of 1.5 g/L. This removal efficiency corresponds to a UED of 7.77 kWh/kg, a $UEMD_{Fe}$ of 0.92 kg/kg and a $UEMD_{Al}$ of 0.94 kg/kg. A further processing up to 35 min led to an insignificant increase in removal efficiency, that is, 96.5%. However, the UED response increased by 46.6%, while $UEMD_{Fe}$ and $UEMD_{Al}$ increased by 20.6% and 43.6%, respectively. Hence, under these conditions the proper EC/GAC processing time is about 25 min.

As shown in our previous work [14], the influence of GAC dose is best pinpointed at low values of current density. The present study aimed at evaluating the influence of this factor on a wider range of GAC dose and Fig. 3b shows the effect of GAC dose at a relatively high value of current

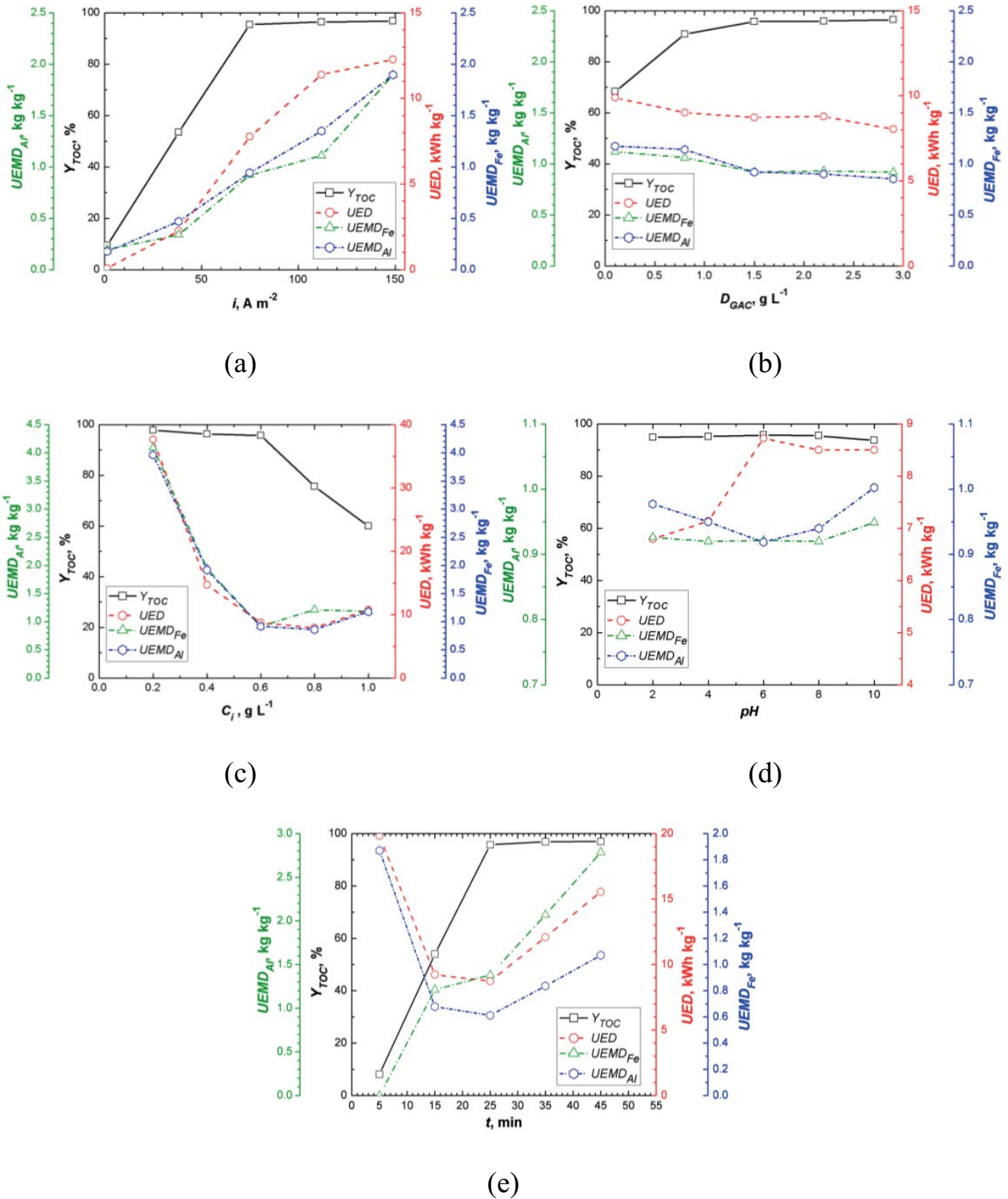


Fig. 3. Variation of the four responses as a function of (a) i ($D_{GAC} = 1.5$ g/L; $C_i = 0.6$ g/L; pH = 6; $t = 25$ min), (b) D_{GAC} ($i = 75.13$ A/m²; $C_i = 0.6$ g/L; pH = 6; $t = 25$ min), (c) C_i ($i = 75.13$ A/m²; $D_{GAC} = 1.5$ g/L; pH = 6; $t = 25$ min), (d) pH ($i = 75.13$ A/m²; $D_{GAC} = 1.5$ g/L; $C_i = 0.6$ g/L; $t = 25$ min), and (e) GAC/EC time, t ($i = 75.13$ A/m²; $C_i = 0.6$ g/L; $D_{GAC} = 1.5$ g/L; pH = 6).

density of 75.1 A/m². In this case, the positive effect of GAC dose on the removal efficiency is obvious up to 1.5 g/L of GAC. One has also to take into account that this dose might be lower for instance at higher values of current density, or might be higher for higher values of initial dye concentration. Due to the synergetic effect of adding GAC in the EC system, the specific responses are also positively influenced. Thus, an increase in GAC dose leads to lower consumptions of electrical energy and electrode materials.

By varying the initial concentration of dye, the removal efficiency decreased slightly with the increase in dye concentration up to 0.6 g/L, while the consumption responses decreased strongly. At higher values of dye concentration, the removal efficiency decreased significantly and consumption responses remained at almost the same level, as shown in Fig. 3c.

In a previous study addressing the removal of AB74 by conventional EC, carried out in the absence of the GAC material, it was shown that the pH has a significant effect only at low values of current density and time [24]. However, in this earlier study, the pH value ranges from 5 to 9 was rather limited and it was found that an acid pH favored the decolorization process. In the present study, although the influence of initial pH was investigated in a very wide range, from 2 to 10, by adding 0.1 N NaOH or 0.1 N H₂SO₄ solutions, it was observed that it had no significant effect on the responses (Fig. 3d).

Fig. 3e shows that EC/GAC time has a strong effect on the responses. As expected, the removal efficiency increased strongly with time up to 25 min, while the specific consumption responses pinpoint the presence of a minimum, excepting the UEMD_{Fe} response. This is due to the fact that in the APC mode, during the first 5 min of operation, iron-based electrodes play the role of cathode, that is, no electrode dissolution takes place.

The amount and appropriateness of the available training data are important factors for obtaining accurate models. The experimental data sets used in this work fulfilled both criteria: a considerable number of experimental data (243 data) were obtained from the EC/GAC coupling processes investigated and the chosen conditions cover the whole domain of interest (experimental domain).

A MLP (5:10:8:4) – feed-forward neural network using a Levenberg–Marquardt learning algorithm with five variables as inputs (current density, GAC dose, concentration of Acid Blue 74, initial pH and EC time), two hidden layers with 10 and 18 neurons, respectively, and four output variables (TOC removal efficiency of the process, electrical energy, Fe and Al doses) and with an average error of 8.37% and a correlation of 0.9731 in the validation stage (with a ratio of 80:20 for training and validation, respectively) was designed to model the EC process applied on a pollutant (Acid Blue 74). The optimization problem is designed to obtain minimum final values of unit energy demand, Al and Fe consumption and a high efficiency of the process, related to the optimal working parameters represented by the inputs of the neural model. The optimization procedure was applied separately considering five objective functions with different degrees of freedom.

GAs were used to determine the optimum operational conditions leading to the maximum efficiency of the electrocoagulation process.

The optimization problem is formulated as follows:

What are the optimal operating parameters (current density, GAC, pollutant concentration, pH and time) necessary to obtain the imposed values for Y_{TOC} , UEMD_{Fe}, UEMD_{Al} and UED responses?

In the present case, the optimization problem includes the best NN model obtained, MLP (5:10:8:4) represented as:

$$\text{ANN [Inputs: } i, D_{\text{GAC}}, C_i, \text{pH}_i, t; \text{Outputs: } Y_{\text{TOC}}, \text{Fe, Al, UED} \quad (5)$$

The vector of control variables, u , has the components:

$$u = [\text{current density, GAC, pollutant concentration, pH, time}] \quad (6)$$

An admissible control input u^* should be formed in such a way that the performance index, J , defined by the following equations, is minimized or maximized:

$$J_1 = w_1 \cdot \left(\frac{1}{Y_{\text{TOC}}} \right)^2 + w_2 \cdot \text{UEMD}_{\text{Fe}}^2 + w_3 \cdot \text{UEMD}_{\text{Al}}^2 + w_4 \cdot \text{UED}^2 \quad (7)$$

$$J_2 = w_1 \cdot \left(1 - \frac{Y_{\text{TOC}}}{Y_{\text{TOC}}d} \right)^2 + w_2 \cdot \text{UEMD}_{\text{Fe}}^2 + w_3 \cdot \text{UEMD}_{\text{Al}}^2 + w_4 \cdot \text{UED}^2 \quad (8)$$

$$J_3 = w_1 \cdot \left(1 - \frac{Y_{\text{TOC}}}{Y_{\text{TOC}}d} \right)^2 + w_2 \cdot \left(1 - \frac{\text{UEMD}_{\text{Fe}}d}{\text{UEMD}_{\text{Fe}}} \right)^2 + w_3 \cdot \text{UEMD}_{\text{Al}}^2 + w_4 \cdot \text{UED}^2 \quad (9)$$

$$J_4 = w_1 \cdot \left(1 - \frac{Y_{\text{TOC}}}{Y_{\text{TOC}}d} \right)^2 + w_2 \cdot \text{UEMD}_{\text{Fe}}^2 + w_3 \cdot \left(1 - \frac{\text{UEMD}_{\text{Al}}d}{\text{UEMD}_{\text{Al}}} \right)^2 + w_4 \cdot \text{UED}^2 \quad (10)$$

$$J_5 = w_1 \cdot \left(\frac{1}{Y_{\text{TOC}}} \right)^2 + w_2 \cdot \left(1 - \frac{\text{UEMD}_{\text{Fe}}d}{\text{UEMD}_{\text{Fe}}} \right)^2 + w_3 \cdot \text{UEMD}_{\text{Al}}^2 + w_4 \cdot \text{UED}^2 \quad (11)$$

$$J_6 = w_1 \cdot \left(1 - \frac{Y_{\text{TOC}}}{Y_{\text{TOC}}d} \right)^2 + w_2 \cdot \text{UEMD}_{\text{Fe}}^2 + w_3 \cdot \left(1 - \frac{\text{UEMD}_{\text{Al}}d}{\text{UEMD}_{\text{Al}}} \right)^2 + w_4 \cdot \left(1 - \frac{\text{UED}d}{\text{UED}} \right)^2 \quad (12)$$

$$J_7 = w_1 \cdot \left(\frac{1}{Y_{\text{TOC}}} \right)^2 + w_2 \cdot \left(1 - \frac{\text{UEMD}_{\text{Fe}}d}{\text{UEMD}_{\text{Fe}}} \right)^2 + w_3 \cdot \text{UEMD}_{\text{Al}}^2 + w_4 \cdot \left(1 - \frac{\text{UED}d}{\text{UED}} \right)^2 \quad (13)$$

Based on the preliminary tests and in order to determine the performance of GAC/EC process in radically different

conditions, and to emphasize the adaptability of this treatment technique to various effluents, the constraints imposed on the multi-objective optimization problem are:

$$\begin{aligned}
 &u_{\min} \leq u \leq u_{\max} \\
 &1.37 \leq \text{current density} \leq 148.91 \text{ A/m}^2 \\
 &0.1 \leq \text{GAC} \leq 2.9 \text{ g/L} \\
 &0.2 \leq \text{pollutant concentration} \leq 1 \text{ g/L} \\
 &2 \leq \text{pH} \leq 10 \\
 &2 \leq \text{time} \leq 150 \text{ min}
 \end{aligned}
 \tag{14}$$

Current density was ranged in the interval 1.365–148.91 A/m², GAC dose from 0.1 to 2.9 g/L, initial AB74 concentration from 0.2 to 1 g/L, initial pH from 2 to 10, and GAC/EC time from 5 to 45 min.

The GA fitness function is the objective function of the optimization problem in many situations [Eqs. (7)–(13)] affected by the constraints (14). Optimization results are the values of decision variables (time, current density, GAC, pH and pollutant concentration) leading to a minimum or maximum of the objective function parameters.

The optimization strategy based on an ANN model and GA as solving technique is shown schematically in Fig. 4.

The method is based on an iterative calculus performed using GA in order to establish the optimal values for decision variables (time, current density, GAC, pH and pollutant concentration) that are the inputs for the NN model and the optimal weights corresponding to each of the four outputs. Applying these inputs, the NN computes the final values of Y , $U\text{EMD}_{\text{Fe}}$, $U\text{EMD}_{\text{Al}}$ and $U\text{ED}$ which could be compared with the desired value in a few cases [Eqs. (4)–(9)]: Y_d , $U\text{EMD}_{\text{Fe},d}$, $U\text{EMD}_{\text{Al},d}$ or $U\text{ED}_d$ depending

on the problem addressed. When the two values are identical or there is a very slight difference between them, the task of the optimization, represented by the minimum of the objective function, J , is achieved.

Generally, the optimization results are influenced by the control parameters of the GA: size of the initial population (pop), number of generations (gen), crossover rate (cross) and mutation rate (mut). A series of runs were performed with different values for these parameters.

In order to select the best GA control parameters, many situations were tested with cross values varying between 0.2 and 2 and mut between 0.001 and 1. The optimized GA parameters in order to ensure accurate prediction results were: dimension of population = 600, generation = 100, cross = 0.9 and mut = 0.03.

Fig. 5 presents several examples corresponding to the situation of Eq. (7) correlated with the limits from Eq. (14) where the parameter Y_{TOC} was maximized and the values of $U\text{EMD}_{\text{Fe}}$, $U\text{EMD}_{\text{Al}}$ and $U\text{ED}$ were minimized. In another considered case, a value for GAC = 2.9 g/L was imposed over the studied range as can be seen from Eq. (14), the results are shown in Table 1.

One of the main goals of the NN-GA approach was to optimize the EC/GAC coupling process. Six optimization cases were considered. Table 1 presents the first three cases differentiated by the imposed constraint, that is, the TOC removal efficiency, for certain values of initial dye concentration in the entire experimental region investigated.

Due to the significant increase in energy and electrode material consumption, a maximum value of 97% was considered for the TOC removal efficiency. Three different levels of TOC removal efficiency were considered 97%, 90% and 80%, respectively.

At first glance, for all three cases considered (different targeted values of removal efficiency), the importance

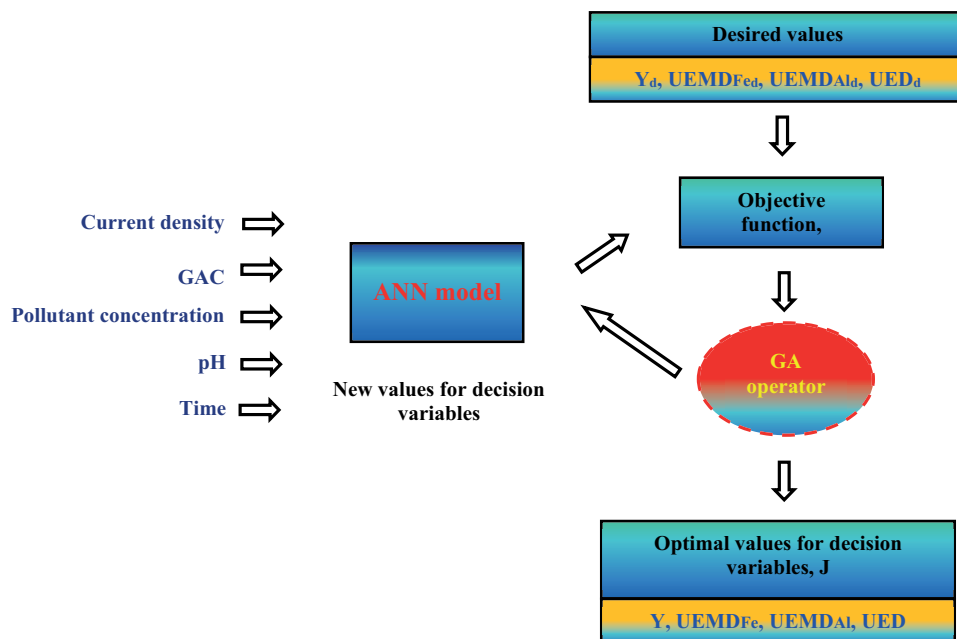


Fig. 4. Optimization strategy based on ANN-GA.

Table 1
Optimizations performed with different values of GA control parameters

No.	Case number	C_i g/L	i A/m ²	pH _{<i>i</i>} –	D_{GAC} g/L	t min	Y_{TOC} %	UEMD _{Fe} kg/kg	UEMD _{Al} kg/kg	UED kWh/kg	EOC €/m ³	Objective function × 10 ³
1		0.2	86.899	4.34	0.884	18.83	97	1.098	1.037	10.169	0.840	0.412
2	Case #1	0.6	83.652	7.93	2.208	27.57	97	0.687	0.508	5.400	1.428	4.159
3		1	82.779	8.89	2.401	30.67	97	0.544	0.421	4.398	1.599	0.374
4		0.2	92.750	2.81	0.931	16.29	90	0.940	1.016	10.01	0.876	3.174
5	Case #2	0.6	83.850	7.99	2.146	24.67	90	0.603	0.471	5.013	1.266	1.922
6		1	82.620	8.34	2.528	27.42	90	0.536	0.436	4.203	1.399	6.322
7		0.2	87.930	4.73	1.147	13.79	80	0.714	0.827	8.739	0.544	8.191
8	Case #3	0.6	46.350	7.04	2.495	33.20	80	0.475	0.342	2.318	0.821	0.001
9		1	82.380	7.64	2.672	23.75	80	0.514	0.449	3.974	1.168	3.978

Table 2
Optimizations performed with different values of GA control parameters under the constraint of the highest dose of GAC = 2.9 g/L

No	Case number	C_i g/L	i A/m ²	pH _{<i>i</i>} –	t min	Y_{TOC} %	UEMD _{Fe} kg/kg	UEMD _{Al} kg/kg	UED kWh/kg	EOC €/m ³	Objective function × 10 ³
1		0.2	82.884	2.57	18.22	97	1.365	1.582	9.207	1.082	2.280
2	Case #4	0.6	86.478	7.00	25.53	97	0.792	0.590	5.195	1.464	3.525
3		1	86.183	7.03	27.36	97	0.63	0.525	4.255	1.448	1.003
4		0.2	93.091	3.72	14.92	90	1.195	1.503	10.156	0.885	9.143
5	Case #5	0.6	84.216	7.91	23.19	90	0.704	0.571	4.712	1.317	1.388
6		1	85.175	7.08	25.32	90	0.6	0.514	4.097	1.315	2.441
7		0.2	92.151	2.96	12.33	80	0.978	1.472	9.044	0.787	5.845
8	Case #6	0.6	42.447	5.48	34.21	80	0.543	0.351	2.008	0.804	0.989
9		1	85.459	6.97	22.43	80	0.554	0.509	3.968	1.148	8.570

of the GAC dose increased with the initial concentration of model pollutant. Therefore, higher GAC doses are suitable for high-loaded wastewater effluents. The treatment duration also increased with the initial concentration of model pollutant. The initial pH had a marginal influence, with the optimal value changing from acidic at low values of initial concentration to slightly alkaline at the highest value of initial concentration. This may be due to an increase in the significance of the adsorption process on the overall EC/GAC treatment process.

Table 2 shows the results obtained for the multi-objective optimization of the EC/GAC coupling process by imposing the highest GAC dose.

Imposing the highest value of GAC dose, the observations corresponding to the optimal values presented in Table 1 are still valid for cases #4–6: treatment duration increased with the initial concentration of model pollutant, and the optimal value of the initial pH changed from acidic to alkaline when increasing the initial concentration of pollutant. Moreover, a general, albeit slight, decrease in specific energy consumption and electrode materials was obtained.

4. Electrical operating costs

According to the EU economic data collected for 2022, the average price of electrical energy for industrial use was

0.2 €/kWh, whereas the prices of mild steel and aluminum were estimated at 1.0 and 2.0 €/kg respectively.

Electrical operational costs (EOCs) consider the costs of electrical energy and electrode material consumed in relation to the amount of pollutant removed. The EOC values were calculated according to Eq. (4).

Comparing the treatment costs of a solution containing 0.1 g/L AB74, at an equivalent cost per kWh, Tabaraki et al. [35] reported estimations of 1.5 €/m³ for Fenton (99% removal efficiency) and 1.7 €/m³ for electro-Fenton (98% removal efficiency), under optimal operating conditions, in batch mode. They also achieved a significantly lower treatment cost by means of biosorption process, reporting 0.27 €/m³, with the drawback of a removal efficiency of only 30%.

Tanyol et al. [3] conducted an optimization study of IC removal (0.02 g/L) by conventional EC using iron electrodes. Under optimal conditions, they reported an equivalent cost of 1.5 €/m (based on the cost of 0.2 €/kWh) corresponding to a value of 82.55% for RE.

According to the local optimum found for case #1, treating an aqueous solution of 0.2 g/L of dye at 86.9 A/m², and adding 0.88 g/L of GAC dose, a removal efficiency of 97% after about 18.83 min was experimentally validated in the ±1.5% range. This corresponds to an EOC of 0.84 €/m³ of pollutant removed. Under these conditions, it is important to note that the cost of energy is about 0.38 €/m³.

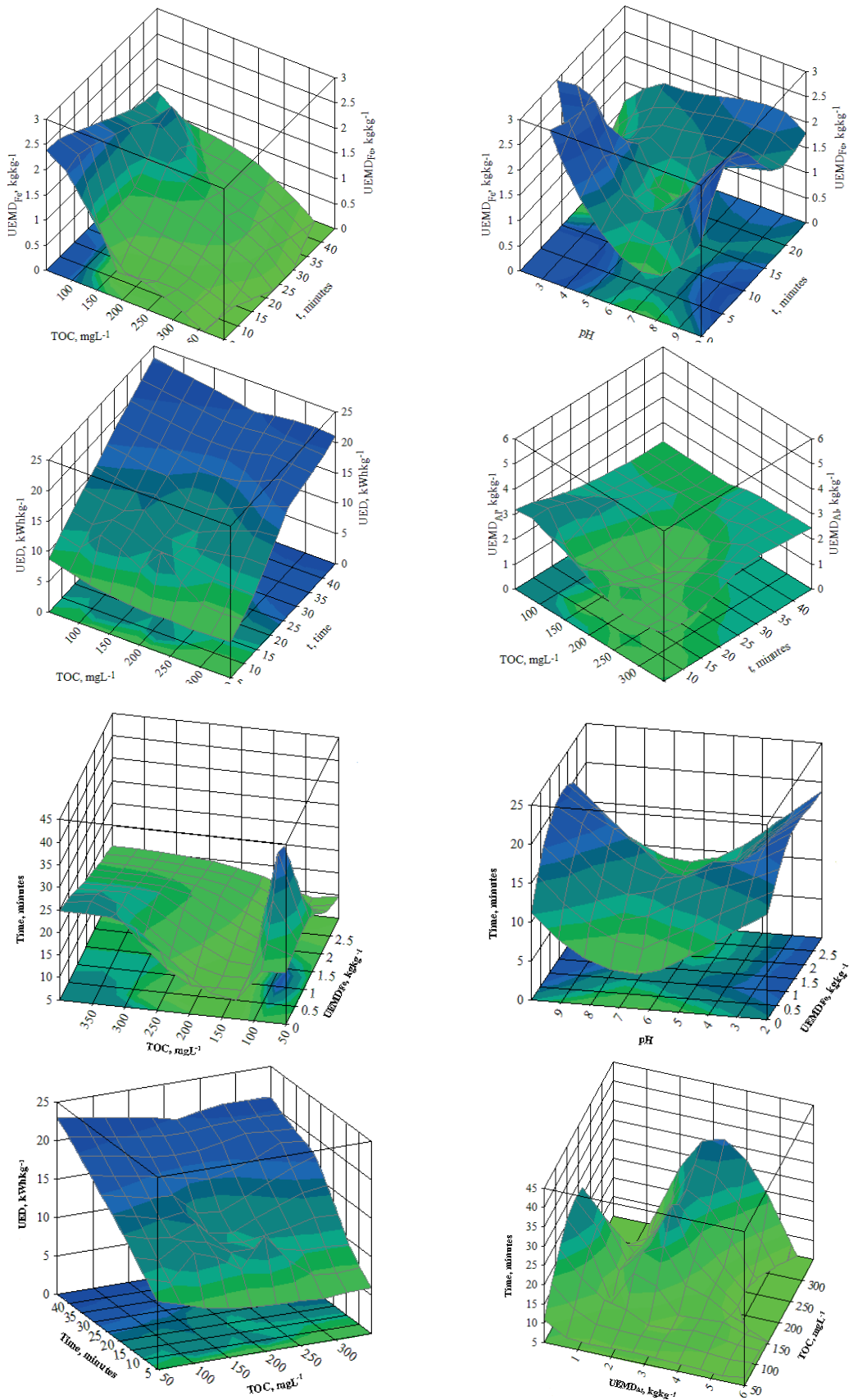


Fig. 5. Influence of the four parameters obtained in the conditions of Eq. (8).

For case #2 and 0.2 g/L of dye and an acid pH value of 2.81, a slightly longer treatment duration corresponds to an EOC 1.01 €/kg of pollutant removed and 0.88 €/m³.

The most efficient EOC values in relation to the pollutant content were obtained for simulated high-loaded effluents. Thus, in case#1 and 1 g/L of dye, the EOC was 0.88 €/kg.

The lowest values of EOC in relation to the volume of treated effluent were achieved in case#6, targeting a removal efficiency not higher than 80%.

In future work the costs of adding GAC to EC systems will be considered. The GAC-enhanced EC system will be operated continuously. The enhancement of the GAC/EC coupling system by means of powder activated carbon will also be addressed.

5. Conclusions

This paper presented a new approach of EC-based techniques meant to maximize removal efficiency and minimize energy and electrode material consumptions. The main goal was to combine in a novel manner a hybrid structure between a neural network model and a genetic algorithm so as to develop an efficient and effective multi-objective optimization procedure.

It was shown that the GAC-enhanced EC process is strongly affected by current density, process duration and initial dye concentration. The effect of GAC dose on the performance of the coupling process was also highlighted.

TOC removal efficiency and the specific consumptions of electrical energy and electrode materials (aluminum and iron based) were considered as process responses.

We have considered in the optimization approach the electrode material consumption, which proved to be a very important cost factor for this treatment method. Several optimization case studies were discussed by assuming different constraints. The efficient use of GAC/EC coupling provides significant reductions in energy and material consumptions.

Thus, maximizing the removal efficiency, it is possible to obtain a 97% TOC removal efficiency for a 0.2 g/L of dye solution by applying a current density of 86.9 A/m² for only 18.83 min and adding a GAC dose of 0.88 g/L. It was determined that in order to achieve this removal efficiency, specific consumptions of energy of 10.17 kWh/kg, iron of 1.098 kg/kg and aluminum of 1.037 kg/kg are required. According to our estimations, these consumptions correspond to a total EOC of 0.84 €/m³.

References

- [1] A. Kothai, C. Sathishkumar, R. Muthupriya, K. Siva Sankar, R. Dharchana, Experimental investigation of textile dyeing wastewater treatment using aluminium in electro coagulation process and Fenton's reagent in advanced oxidation process, *Mater. Today: Proc.*, 45 (2020) 1411–1416.
- [2] G. Fischer-Colbrie, J. Maier, K.H. Robra, G.M. Guebitz, In: E. Lichtfouse, J. Schwarzbauer, D. Robert, *Green Chemistry and Pollutants in Ecosystems*, Springer, Berlin, 2005, pp. 289–294.
- [3] M. Tanyol, N.C. Yildirim, D. Alparslan, Electrocoagulation induced treatment of indigo carmine textile dye in an aqueous medium: the effect of process variables on efficiency evaluated using biochemical response of *Gammarus pulex*, *Environ. Sci. Pollut. Res.*, 28 (2021) 55315–55329.
- [4] A.G.S. Prado, J.D. Torres, E.A. Faria, S.C.L. Dias, Comparative adsorption studies of indigo carmine dye on chitin and chitosan, *J. Colloid Interface Sci.*, 277 (2004) 43–47.
- [5] O. Tahiri Alaoui, Q.T. Nguyen, C. Mbareck, T. Rhallou, Elaboration and study of poly(vinylidene fluoride)-anatase TiO₂ composite membranes in photocatalytic degradation of dyes, *Appl. Catal., A*, 358 (2009) 13–20.
- [6] K. Rajeshwar, J.G. Ibanez, *Environmental Electrochemistry*, Academic Press, UK, 1997.
- [7] A. Azanaw, B. Birlie, B. Teshome, M. Jemberie, Textile effluent treatment methods and eco-friendly resolution of textile wastewater, *Case Stud. Chem. Environ. Eng.*, 6 (2022) 100230, doi: 10.1016/j.csee.2022.100230.
- [8] M. Bayramoglu, M. Eyvaz, M. Kobya, Treatment of the textile wastewater by electrocoagulation economical evaluation, *Chem. Eng. J.*, 128 (2007) 155–161.
- [9] M. Kobya, M. Bayramoglu, M. Eyvaz, Techno-economical evaluation of electrocoagulation for the textile wastewater using different electrode connections, *J. Hazard. Mater.*, 148 (2007) 311–318.
- [10] F.E. Titchou, H. Zazou, H. Afanga, J. El Gaayda, R.A. Akbour, M. Hamdani, Removal of persistent organic pollutants (POPs) from water and wastewater by adsorption and electrocoagulation process, *Groundwater Sustainable Dev.*, 13 (2021) 100575, doi: 10.1016/j.gsd.2021.100575.
- [11] M. Yousuf, A. Mollah, J.A.G. Gomes, K.K. Das, D.L. Cocke, Electrochemical treatment of Orange II dye solution—use of aluminum sacrificial electrodes and floc characterization, *J. Hazard. Mater.*, 174 (2010) 851–858.
- [12] M. Bayramoglu, M. Kobya, O.T. Can, M. Sozbir, Operating cost analysis of electrocoagulation of textile dye wastewater, *Sep. Purif. Technol.*, 37 (2004) 117–125.
- [13] V. Katheresan, J. Kannedo, S.Y. Lau, Efficiency of various recent wastewater dye removal methods: a review, *J. Environ. Chem. Eng.*, 6 (2018) 4679–4697.
- [14] M.S. Secula, B. Cagnon, T. Ferreira de Oliveira, O. Chedeville, H. Fauduet, Removal of acid dye from aqueous solutions by electrocoagulation/GAC adsorption coupling: kinetics and electrical operating costs, *J. Taiwan Inst. Chem. Eng.*, 43 (2012) 767–775.
- [15] U. Ratt, R. Minks, Overview of wastewater treatment and recycling in the textile processing industry water, *Sci. Technol.*, 40 (1999) 137–144.
- [16] J. Leboreiro, J. Acevedo, Processes synthesis and design of distillation sequence using modular simulators: a genetic algorithm framework, *Comput. Chem. Eng.*, 28 (2004) 1223–1236.
- [17] C. Guria, P.K. Bhattacharza, S.K. Gupta, Multi-objective optimization of reverse osmosis desalination units using different adaptations of the non-dominated sorting genetic algorithm (NSGA), *Comput. Chem. Eng.*, 29 (2005) 1977–1995.
- [18] W.H. Jang, J. Hahn, R.K. Hall, Genetic/quadratic search algorithm for plant economic optimizations using a process simulator, *Comput. Chem. Eng.*, 30 (2005) 285–294.
- [19] S. Katare, A. Bhan, J. Caruthers, W.N. Delgass, A hybrid genetic algorithm for efficient parameter estimation of large kinetic models, *Comput. Chem. Eng.*, 28 (2004) 2569–258.
- [20] S. Curteanu, C.G. Piuleac, K. Godini, G. Azaryan, Modeling of electrolysis process in wastewater treatment using different types of neural networks, *Chem. Eng. J.*, 172 (2011) 267–276.
- [21] G.D. Suditu, M. Secula, C.G. Piuleac, S. Curteanu, I. Poullos, Genetic algorithms and neural networks-based optimization applied to the wastewater decolorization by photocatalytic reaction, *Rev. Chim.*, 7 (2008) 816–825.
- [22] C.G. Piuleac, S. Curteanu, M. Cazacu, Optimization by NN-GA technique of the metal complexing process – potential application in wastewater treatment, *Environ. Eng. Manage. J.*, 9 (2010) 239–247.
- [23] P.S. Georgiadou, I.A. Papazoglou, C.T. Kiranoudis, N.C. Markatos, Multi-objective evolutionary emergency response optimization for major accidents, *J. Hazard. Mater.*, 178 (2010) 792–803.

- [24] M.S. Secula, I. Cretescu, S. Petrescu, An experimental study of Indigo Carmine dye removal from aqueous solutions by electrocoagulation, *Desalination*, 277 (2011) 227–235.
- [25] M.S. Secula, L. Zaleschi, C.S. Stan, I. Mamaliga, Effects of electric current type and electrode configuration on the removal of Indigo Carmine from aqueous solutions by electrocoagulation in a batch reactor, *Desal. Water Treat.*, 52 (2014) 6135–6144.
- [26] M. Eyvaz, M. Kirlaroglu, T.S. Aktas, E. Yuksel, The effects of alternating current electrocoagulation on dye removal from aqueous solutions, *Chem. Eng. J.*, 153 (2009) 16–22.
- [27] Ö. Apaydin, U. Kurt, M.T. Gönüllü, An investigation on the treatment of tannery wastewater by electrocoagulation, *Global NEST J.*, 11 (2009) 546–555.
- [28] F.R. Espinoza-Quinones, M.M.T. Fornari, A.N. Módenes, S.M. Palácio, F.G. da Silva Jr., N.A.D. Szymanski, N. Kroumov, D.E.G. Trigueros, Pollutant removal from tannery effluent by electrocoagulation, *Chem. Eng. J.*, 151 (2009) 59–65.
- [29] J.C. Donini, J. Kan, J. Szynekarczuk, T.A. Hassan, K.L. Kar, Operating cost of electrocoagulation, *Can. J. Chem. Eng.*, 72 (1994) 1007–1012.
- [30] M.S. Secula, I. Cretescu, S. Petrescu, Electrocoagulation treatment of sulfide wastewater in a batch reactor: effect of electrode material on the electrical operating costs, *Environ. Eng. Manage. J.*, 11 (2012) 1485–1491.
- [31] M.Y.A. Mollah, P. Morkovsky, J.A.G. Gomes, M. Kesmez, J. Pargad, D.L. Cocke, Fundamentals, present and future perspectives of electrocoagulation, *J. Hazard. Mater.*, 114 (2004) 199–210.
- [32] L. Wang, L. Zhang, D.Z. Zheng, An effective hybrid genetic algorithm for flow shop scheduling with limited buffers, *Comput. Oper. Res.*, 33 (2006) 2969–2971.
- [33] C.M. Silva, E.C. Biscaia, Genetic algorithm development for multi-objective optimization of batch free-radical polymerization reactors, *Comput. Chem. Eng.*, 27 (2003) 1329–1344.
- [34] K. Deb, *Multi-objective Optimization Using Evolutionary Algorithms*, Wiley, Chichester, UK 2001.
- [35] R. Tabaraki, S. Zadkhast, A. Najaf, V.R. Moghaddam, Performance and cost analysis of dye wastewater treatment by Fenton, electro-Fenton, and biosorption: Box–Behnken experimental design and response surface methodology, *Biomass Convers. Biorefin.*, (2022), doi: 10.1007/s13399-022-02809-2.

Supporting information

Table S1

Experimental data

No. Crt.	Test	i A/m ²	D_{GAC} g/L	C_i g/L	pH _{<i>i</i>} –	t min	Y_{TOC} %	UEMD _{Fe} kg/kg	UEMD _{Al} kg/kg	UED kWh/kg
1	R-1	148.91	1.5	0.6	6	5	10.40	8.71	0.10	4.52
2	R-1	148.91	1.5	0.6	6	10	95.17	5.35	0.92	0.70
3	R-1	148.91	1.5	0.6	6	15	95.50	7.72	0.96	1.20
4	R-1	148.91	1.5	0.6	6	20	96.92	9.99	1.83	1.39
5	R-1	148.91	1.5	0.6	6	25	96.87	12.28	1.90	1.90
6	R-1	148.91	1.5	0.6	6	30	96.89	14.75	2.77	2.11
7	R-1	148.91	1.5	0.6	6	35	96.93	16.93	2.87	2.62
8	R-1	148.91	1.5	0.6	6	40	96.95	19.37	3.73	2.85
9	R-1	148.91	1.5	0.6	6	45	96.96	21.49	3.86	3.37
10	R-1	75.14	1.5	0.6	6	5	7.76	18.42	0.00	2.99
11	R-1	75.14	1.5	0.6	6	10	22.25	13.68	1.94	1.47
12	R-10	75.14	1.5	0.6	6	15	23.81	18.64	1.83	2.37
13	R-10	75.14	1.5	0.6	6	20	95.04	6.35	0.92	0.70
14	R-10	75.14	1.5	0.6	6	25	95.48	7.77	0.92	0.94
15	R-10	75.14	1.5	0.6	6	30	96.91	9.31	1.37	1.03
16	R-10	75.14	1.5	0.6	6	35	96.93	10.73	1.37	1.29
17	R-10	75.14	1.5	0.6	6	40	96.99	12.37	1.84	1.39
18	R-10	75.14	1.5	0.6	6	45	96.99	13.79	1.85	1.65
19	R-11	38.25	0.8	0.4	4	5	10.74	7.67	0.08	2.09
20	R-11	38.25	0.8	0.4	4	10	18.63	9.85	2.17	1.76
21	R-11	38.25	0.8	0.4	4	15	20.88	12.70	2.07	2.66
22	R-11	38.25	0.8	0.4	4	20	62.19	5.85	1.31	1.06
23	R-11	38.25	0.8	0.4	4	25	89.08	5.00	0.97	1.00
24	R-11	38.25	0.8	0.4	4	30	93.83	5.81	1.32	1.07
25	R-11	38.25	0.8	0.4	4	35	94.42	6.64	1.38	1.31
26	R-11	38.25	0.8	0.4	4	40	94.72	7.67	1.76	1.43
27	R-11	38.25	0.8	0.4	4	45	94.73	8.53	1.86	1.68

(continued)

Table S1 Continued

No. Crt.	Test	i A/m ²	D_{GAC} g/L	C_i g/L	pH _{i} –	t min	Y_{TOC} %	UEMD _{Fe} kg/kg	UEMD _{Al} kg/kg	UED kWh/kg
28	R-12	112.02	0.8	0.4	4	5	12.13	44.89	0.00	4.82
29	R-12	112.02	0.8	0.4	4	10	92.18	12.35	1.23	0.88
30	R-12	112.02	0.8	0.4	4	15	92.15	18.12	1.24	1.52
31	R-12	112.02	0.8	0.4	4	20	94.72	23.85	2.42	1.73
32	R-12	112.02	0.8	0.4	4	25	94.69	29.37	2.43	2.37
33	R-12	112.02	0.8	0.4	4	30	94.69	35.50	3.67	2.62
34	R-12	112.02	0.8	0.4	4	35	94.71	41.01	3.69	3.61
35	R-12	112.02	0.8	0.4	4	40	94.71	47.13	4.94	3.53
36	R-12	112.02	0.8	0.4	4	45	94.72	52.64	4.97	4.19
37	R-13	38.25	0.8	0.8	4	5	7.08	0.02	0.00	1.55
38	R-13	38.25	0.8	0.8	4	10	9.10	0.06	2.15	1.73
39	R-13	38.25	0.8	0.8	4	15	15.97	0.04	1.23	1.69
40	R-13	38.25	0.8	0.8	4	20	24.53	0.12	1.61	1.30
41	R-13	38.25	0.8	0.8	4	25	24.95	0.06	1.59	1.73
42	R-13	38.25	0.8	0.8	4	30	58.76	0.18	1.02	0.82
43	R-13	38.25	0.8	0.8	4	35	59.80	0.08	1.01	1.00
44	R-13	38.25	0.8	0.8	4	40	66.42	0.24	1.22	0.98
45	R-13	38.25	0.8	0.8	4	45	66.72	0.10	1.22	1.15
46	R-14	112.02	0.8	0.8	4	5	7.91	35.42	0.00	3.75
47	R-14	112.02	0.8	0.8	4	10	25.43	22.95	2.25	1.62
48	R-14	112.02	0.8	0.8	4	15	27.82	30.71	2.07	2.57
49	R-14	112.02	0.8	0.8	4	20	40.84	28.24	2.83	2.04
50	R-14	112.02	0.8	0.8	4	25	40.36	35.26	2.88	2.82
51	R-14	112.02	0.8	0.8	4	30	95.98	17.93	1.83	1.31
52	R-14	112.02	0.8	0.8	4	35	96.41	20.62	1.83	1.63
53	R-14	112.02	0.8	0.8	4	40	97.06	23.54	2.43	1.75
54	R-14	112.02	0.8	0.8	4	45	96.79	26.32	2.45	2.08
55	R-15	38.25	0.8	0.4	8	5	7.87	10.79	0.01	2.73
56	R-15	38.25	0.8	0.4	8	10	18.99	9.77	2.03	1.63
57	R-15	38.25	0.8	0.4	8	15	20.20	13.31	1.93	2.61
58	R-15	38.25	0.8	0.4	8	20	35.58	10.33	2.19	1.76
59	R-15	38.25	0.8	0.4	8	25	35.81	12.59	2.20	2.37
60	R-15	38.25	0.8	0.4	8	30	94.20	5.85	1.25	1.00
61	R-15	38.25	0.8	0.4	8	35	94.15	6.73	1.27	1.25
62	R-15	38.25	0.8	0.4	8	40	94.77	7.76	1.68	1.35
63	R-15	38.25	0.8	0.4	8	45	94.80	8.64	1.69	1.59
64	R-16	112.02	0.8	0.4	8	5	9.34	61.34	0.43	5.68
65	R-16	112.02	0.8	0.4	8	10	90.73	13.14	1.33	0.78
66	R-16	112.02	0.8	0.4	8	15	92.88	18.76	1.44	1.34
67	R-16	112.02	0.8	0.4	8	20	94.74	24.84	2.58	1.50
68	R-16	112.02	0.8	0.4	8	25	94.69	30.58	2.81	2.08
69	R-16	112.02	0.8	0.4	8	30	94.77	36.91	3.90	2.27
70	R-16	112.02	0.8	0.4	8	35	94.74	42.64	4.23	3.12
71	R-16	112.02	0.8	0.4	8	40	94.79	48.97	5.26	3.06
72	R-16	112.02	0.8	0.4	8	45	94.79	54.70	5.69	3.66
73	R-17	38.25	0.8	0.8	8	5	4.73	9.33	0.00	2.28
74	R-17	38.25	0.8	0.8	8	10	10.49	9.30	1.87	1.47
75	R-17	38.25	0.8	0.8	8	15	12.70	11.10	1.55	2.08
76	R-17	38.25	0.8	0.8	8	20	21.85	8.81	1.81	1.42

(continued)

Table S1 Continued

No. Crt.	Test	i A/m ²	D_{GAC} g/L	C_i g/L	pH _{i} –	t min	Y_{TOC} %	UEMD _{Fe} kg/kg	UEMD _{Al} kg/kg	UED kWh/kg
77	R-17	38.25	0.8	0.8	8	25	25.76	9.15	1.55	1.64
78	R-17	38.25	0.8	0.8	8	30	57.11	5.02	1.05	0.83
79	R-17	38.25	0.8	0.8	8	35	57.48	5.74	1.05	1.02
80	R-17	38.25	0.8	0.8	8	40	65.19	5.85	1.24	0.97
81	R-17	38.25	0.8	0.8	8	45	64.92	6.55	1.25	1.16
82	R-18	112.02	0.8	0.8	8	5	8.08	35.40	0.00	3.70
83	R-18	112.02	0.8	0.8	8	10	50.88	11.69	1.13	0.82
84	R-18	112.02	0.8	0.8	8	15	52.34	16.63	1.11	1.37
85	R-18	112.02	0.8	0.8	8	20	65.62	17.90	1.77	1.28
86	R-18	112.02	0.8	0.8	8	25	65.08	22.26	1.80	1.77
87	R-18	112.02	0.8	0.8	8	30	96.18	18.22	1.83	1.32
88	R-18	112.02	0.8	0.8	8	35	95.59	21.18	1.85	1.66
89	R-18	112.02	0.8	0.8	8	40	96.90	24.01	2.45	1.77
90	R-18	112.02	0.8	0.8	8	45	96.77	26.83	2.47	2.10
91	R-19	38.25	2.2	0.4	4	5	14.59	6.11	0.00	1.41
92	R-19	38.25	2.2	0.4	4	10	20.37	9.64	1.88	1.42
93	R-19	38.25	2.2	0.4	4	15	26.18	10.85	1.47	1.90
94	R-19	38.25	2.2	0.4	4	20	36.48	10.63	2.12	1.60
95	R-19	38.25	2.2	0.4	4	25	37.97	12.52	2.04	2.10
96	R-19	38.25	2.2	0.4	4	30	94.40	6.14	1.24	0.94
97	R-19	38.25	2.2	0.4	4	35	94.21	7.08	1.25	1.17
98	R-19	38.25	2.2	0.4	4	40	94.82	8.15	1.66	1.26
99	R-19	38.25	2.2	0.4	4	45	94.83	9.08	1.67	1.49
100	R-2	1.37	1.5	0.6	6	5	2.89	0.00	0.01	0.15
101	R-2	1.37	1.5	0.6	6	10	3.71	0.11	0.23	0.17
102	R-2	1.37	1.5	0.6	6	15	4.90	0.09	0.19	0.22
103	R-2	1.37	1.5	0.6	6	20	6.30	0.13	0.27	0.20
104	R-2	1.37	1.5	0.6	6	25	9.53	0.09	0.20	0.18
105	R-2	1.37	1.5	0.6	6	30	9.09	0.14	0.28	0.21
106	R-2	1.37	1.5	0.6	6	35	10.00	0.14	0.28	0.24
107	R-2	1.37	1.5	0.6	6	40	10.90	0.16	0.32	0.23
108	R-2	1.37	1.5	0.6	6	45	12.02	0.15	0.31	0.25
109	R-20	112.02	2.2	0.4	4	5	20.80	27.75	0.00	2.56
110	R-20	112.02	2.2	0.4	4	10	92.62	13.01	1.20	0.77
111	R-20	112.02	2.2	0.4	4	15	93.92	18.88	1.19	1.33
112	R-20	112.02	2.2	0.4	4	20	94.85	25.26	2.38	1.51
113	R-20	112.02	2.2	0.4	4	25	94.76	31.19	2.39	2.09
114	R-20	112.02	2.2	0.4	4	30	94.85	37.71	3.60	2.29
115	R-20	112.02	2.2	0.4	4	35	94.85	43.61	3.62	3.14
116	R-20	112.02	2.2	0.4	4	40	94.85	50.15	4.85	3.09
117	R-20	112.02	2.2	0.4	4	45	94.85	56.05	4.88	3.69
118	R-21	38.25	2.2	0.8	4	5	9.83	4.57	0.00	1.07
119	R-21	38.25	2.2	0.8	4	10	13.68	7.29	1.44	1.09
120	R-21	38.25	2.2	0.8	4	15	17.20	8.38	1.15	1.49
121	R-21	38.25	2.2	0.8	4	20	24.60	8.02	1.61	1.22
122	R-21	38.25	2.2	0.8	4	25	52.81	4.58	0.76	0.78
123	R-21	38.25	2.2	0.8	4	30	60.63	4.86	0.99	0.75
124	R-21	38.25	2.2	0.8	4	35	61.89	5.48	0.98	0.92
125	R-21	38.25	2.2	0.8	4	40	94.64	4.15	0.86	0.65

(continued)

Table S1 Continued

No. Crt.	Test	i A/m ²	D_{GAC} g/L	C_i g/L	pH _{i} –	t min	Y_{TOC} %	UEMD _{Fe} kg/kg	UEMD _{Al} kg/kg	UED kWh/kg
126	R-21	38.25	2.2	0.8	4	45	94.60	4.63	0.86	0.77
127	R-21	112.02	2.2	0.8	4	5	12.46	22.70	0.00	2.38
128	R-22	112.02	2.2	0.8	4	10	56.61	10.37	1.02	0.73
129	R-22	112.02	2.2	0.8	4	15	59.25	14.53	0.98	1.20
130	R-22	112.02	2.2	0.8	4	20	95.80	12.15	1.22	0.87
131	R-22	112.02	2.2	0.8	4	25	96.55	14.89	1.21	1.18
132	R-22	112.02	2.2	0.8	4	30	97.25	17.90	1.81	1.29
133	R-22	112.02	2.2	0.8	4	35	69.26	29.06	2.56	2.27
134	R-22	112.02	2.2	0.8	4	40	97.33	23.79	2.44	1.74
135	R-22	112.02	2.2	0.8	4	45	97.30	26.58	2.46	2.07
136	R-23	38.25	2.2	0.4	8	5	13.88	6.21	0.00	1.50
137	R-23	38.25	2.2	0.4	8	10	21.35	8.91	1.79	1.39
138	R-23	38.25	2.2	0.4	8	15	26.81	10.32	1.44	1.90
139	R-23	38.25	2.2	0.4	8	20	36.04	10.51	2.15	1.66
140	R-23	38.25	2.2	0.4	8	25	90.01	5.18	0.86	0.91
141	R-23	38.25	2.2	0.4	8	30	94.74	6.01	1.24	0.96
142	R-23	38.25	2.2	0.4	8	35	94.77	6.93	1.24	1.19
143	R-23	38.25	2.2	0.4	8	40	94.82	8.02	1.67	1.29
144	R-23	38.25	2.2	0.4	8	45	94.82	8.92	1.68	1.53
145	R-24	112.02	2.2	0.4	8	5	16.33	35.68	0.18	3.22
146	R-24	112.02	2.2	0.4	8	10	90.32	13.47	1.31	0.77
147	R-24	112.02	2.2	0.4	8	15	92.63	19.33	1.38	1.33
148	R-24	112.02	2.2	0.4	8	20	94.51	25.57	2.53	1.48
149	R-24	112.02	2.2	0.4	8	25	94.80	31.43	2.69	2.05
150	R-24	112.02	2.2	0.4	8	30	94.81	38.03	3.82	2.24
151	R-24	112.02	2.2	0.4	8	35	94.81	43.97	4.06	3.08
152	R-24	112.02	2.2	0.4	8	40	94.81	50.58	5.14	3.02
153	R-24	112.02	2.2	0.4	8	45	94.81	56.51	5.45	3.61
154	R-25	38.25	2.2	0.8	8	5	7.57	5.79	0.00	1.40
155	R-25	38.25	2.2	0.8	8	10	12.67	7.70	1.54	1.18
156	R-25	38.25	2.2	0.8	8	15	16.29	8.67	1.21	1.58
157	R-25	38.25	2.2	0.8	8	20	24.16	8.00	1.63	1.25
158	R-25	38.25	2.2	0.8	8	25	52.31	4.53	0.76	0.79
159	R-25	38.25	2.2	0.8	8	30	60.27	4.79	0.99	0.76
160	R-25	38.25	2.2	0.8	8	35	61.00	5.44	0.99	0.93
161	R-25	38.25	2.2	0.8	8	40	94.39	4.07	0.85	0.65
162	R-25	38.25	2.2	0.8	8	45	94.50	4.53	0.86	0.77
163	R-26	112.02	2.2	0.8	8	5	10.11	28.54	0.00	2.95
164	R-26	112.02	2.2	0.8	8	10	55.58	10.79	1.03	0.75
165	R-26	112.02	2.2	0.8	8	15	57.97	15.17	0.99	1.24
166	R-26	112.02	2.2	0.8	8	20	96.03	12.36	1.21	0.87
167	R-26	112.02	2.2	0.8	8	25	96.30	15.22	1.21	1.19
168	R-26	112.02	2.2	0.8	8	30	97.21	18.24	1.81	1.31
169	R-26	112.02	2.2	0.8	8	35	97.18	21.10	1.82	1.63
170	R-26	112.02	2.2	0.8	8	40	97.33	24.23	2.43	1.76
171	R-26	112.02	2.2	0.8	8	45	97.30	27.08	2.45	2.09
172	R-27	75.14	1.5	0.6	6	5	8.13	19.83	0.00	2.81
173	R-27	75.14	1.5	0.6	6	10	51.81	6.60	0.84	0.62
174	R-27	75.14	1.5	0.6	6	15	54.06	9.24	0.81	1.02

(continued)

Table S1 Continued

No. Crt.	Test	i A/m ²	D_{GAC} g/L	C_i g/L	pH ₁ –	t min	Y_{TOC} %	UEMD _{Fe} kg/kg	UEMD _{Al} kg/kg	UED kWh/kg
175	R-27	75.14	1.5	0.6	6	20	95.01	7.14	0.92	0.68
176	R-27	75.14	1.5	0.6	6	25	95.79	8.73	0.92	0.92
177	R-27	75.14	1.5	0.6	6	30	96.93	10.48	1.37	1.01
178	R-27	75.14	1.5	0.6	6	35	96.91	12.10	1.38	1.26
179	R-27	75.14	1.5	0.6	6	40	97.00	13.94	1.85	1.36
180	R-27	75.14	1.5	0.6	6	45	96.99	15.56	1.86	1.61
181	R-3	75.14	0.1	0.6	6	5	14.05	10.61	0.00	1.68
182	R-3	75.14	0.1	0.6	6	10	49.84	6.39	0.87	0.67
183	R-3	75.14	0.1	0.6	6	15	51.37	9.05	0.84	1.12
184	R-3	75.14	0.1	0.6	6	20	63.37	9.95	1.38	1.07
185	R-3	75.14	0.1	0.6	6	25	78.33	9.89	1.12	1.17
186	R-3	75.14	0.1	0.6	6	30	96.54	9.75	1.37	1.06
187	R-3	75.14	0.1	0.6	6	35	96.21	11.27	1.38	1.32
188	R-3	75.14	0.1	0.6	6	40	96.89	12.91	1.84	1.42
189	R-3	75.14	0.1	0.6	6	45	96.76	14.41	1.85	1.69
190	R-4	75.14	1.5	0.2	6	5	85.76	7.48	0.00	1.06
191	R-4	75.14	1.5	0.2	6	10	87.67	15.44	2.02	1.43
192	R-4	75.14	1.5	0.2	6	15	87.80	22.53	2.03	2.48
193	R-4	75.14	1.5	0.2	6	20	87.82	30.61	4.07	2.89
194	R-4	75.14	1.5	0.2	6	25	87.83	37.65	4.09	3.96
195	R-4	75.14	1.5	0.2	6	30	87.82	45.67	6.17	4.38
196	R-4	75.14	1.5	0.2	6	35	87.83	52.99	6.20	6.03
197	R-4	75.14	1.5	0.2	6	40	87.83	61.09	8.31	5.90
198	R-4	75.14	1.5	0.2	6	45	87.83	68.21	8.35	7.01
199	R-5	75.14	2.9	0.6	6	5	11.60	12.63	0.00	1.87
200	R-5	75.14	2.9	0.6	6	10	52.76	5.94	0.82	0.56
201	R-5	75.14	2.9	0.6	6	15	57.18	8.05	0.77	0.90
202	R-5	75.14	2.9	0.6	6	20	96.46	6.52	0.91	0.62
203	R-5	75.14	2.9	0.6	6	25	96.58	8.04	0.92	0.85
204	R-5	75.14	2.9	0.6	6	30	97.01	9.75	1.38	0.93
205	R-5	75.14	2.9	0.6	6	35	97.01	11.27	1.39	1.17
206	R-5	75.14	2.9	0.6	6	40	97.01	13.02	1.85	1.26
207	R-5	75.14	2.9	0.6	6	45	97.01	14.55	1.86	1.50
208	R-6	75.14	1.5	0.6	2	5	9.30	10.60	0.00	3.15
209	R-6	75.14	1.5	0.6	2	10	25.23	9.32	1.72	1.50
210	R-6	75.14	1.5	0.6	2	15	61.21	6.00	0.71	0.99
211	R-6	75.14	1.5	0.6	2	20	94.32	5.48	0.93	0.74
212	R-6	75.14	1.5	0.6	2	25	94.96	6.80	0.93	0.98
213	R-6	75.14	1.5	0.6	2	30	95.37	8.34	1.39	1.07
214	R-6	75.14	1.5	0.6	2	35	95.94	9.62	1.39	1.31
215	R-6	75.14	1.5	0.6	2	40	96.11	11.17	1.86	1.40
216	R-6	75.14	1.5	0.6	2	45	96.43	12.45	1.86	1.65
217	R-7	75.14	1.5	0.6	10	5	4.85	32.36	0.00	4.95
218	R-7	75.14	1.5	0.6	10	10	48.30	6.85	0.91	0.71
219	R-7	75.14	1.5	0.6	10	15	51.51	9.31	0.85	1.14
220	R-7	75.14	1.5	0.6	10	20	93.64	6.94	0.94	0.74
221	R-7	75.14	1.5	0.6	10	25	93.70	8.50	0.95	1.00
222	R-7	75.14	1.5	0.6	10	30	96.34	10.03	1.39	1.09
223	R-7	75.14	1.5	0.6	10	35	96.42	11.54	1.40	1.35

(continued)

Table S1 Continued

No. Crt.	Test	i A/m ²	D_{GAC} g/L	C_i g/L	pH _{i} –	t min	Y_{TOC} %	UEMD _{Fe} kg/kg	UEMD _{Al} kg/kg	UED kWh/kg
224	R-7	75.14	1.5	0.6	10	40	96.69	13.26	1.87	1.46
225	R-7	75.14	1.5	0.6	10	45	96.64	14.79	1.88	1.73
226	R-8	75.14	1.5	1	6	5	10.19	12.30	0.00	1.79
227	R-8	75.14	1.5	1	6	10	18.02	14.77	1.93	1.42
228	R-8	75.14	1.5	1	6	15	21.78	17.76	1.61	2.03
229	R-8	75.14	1.5	1	6	20	58.55	8.97	1.20	0.88
230	R-8	75.14	1.5	1	6	25	59.96	10.76	1.18	1.18
231	R-8	75.14	1.5	1	6	30	80.85	9.69	1.32	0.97
232	R-8	75.14	1.5	1	6	35	81.40	11.11	1.32	1.20
233	R-8	75.14	1.5	1	6	40	96.41	10.82	1.49	1.09
234	R-8	75.14	1.5	1	6	45	96.17	12.11	1.50	1.30
235	R-9	75.14	1.5	0.6	6	5	7.51	20.91	0.00	3.16
236	R-9	75.14	1.5	0.6	6	10	21.93	15.16	1.98	1.54
237	R-9	75.14	1.5	0.6	6	15	24.15	20.08	1.81	2.40
238	R-9	75.14	1.5	0.6	6	20	94.98	6.94	0.92	0.72
239	R-9	75.14	1.5	0.6	6	25	95.99	8.44	0.92	0.97
240	R-9	75.14	1.5	0.6	6	30	96.88	10.14	1.37	1.07
241	R-9	75.14	1.5	0.6	6	35	96.88	11.68	1.38	1.32
242	R-9	75.14	1.5	0.6	6	40	96.95	13.43	1.85	1.44
243	R-9	75.14	1.5	0.6	6	45	96.97	14.94	1.86	1.70